EXPERIMENTAL METHODS FOR IDENTIFYING AIR INFILTRATION HEAT RECOVERY IN BUILDINGS

Mingsheng Liu, Ph.D. David E. Claridge, Ph.D., P.E.

ABSTRACT

This paper presents two methods that can be used to determine the air infiltration heat recovery in buildings: (1) the co-heating method and (2) the short-term average method (STAM). These methods were developed based on fundamental heat transfer principles and experimental research.

INTRODUCTION

When calculating the heating and cooling loads of buildings, it is assumed that the air infiltration energy consumption is the same as that required to heat (or cool) outside air to the indoor conditions. However, the actual air infiltration energy consumption can differ from this value depending on the buildings' characteristics and weather because of the interaction of heat conduction, solar radiation, and air infiltration in the building components (Timusk and Doshi 1986; Timusk et al. 1992; Morisson et al. 1992; Virtanen et al. 1992; Anderlind 1985; Guo and Liu 1985; Claridge and Bhattacharyya 1989; Bhattacharyya and Claridge 1992; Liu and Claridge 1992a, 1992b, 1992c).

To estimate the difference between the energy consumption with and without the interaction noted above, the air infiltration heat exchange effectiveness (IHEE) index was proposed by Claridge and Bhattacharyya (1989). It expresses the difference between total heat flux (E_{cl}), calculated according to the American Society of Heating, Refrigerating and Air-Conditioning Engineers' (ASHRAE) method (ASHRAE 1993), and the total actual measured heat flux (E_{ac}) as a fraction of the classic air infiltration energy consumption:

$$\text{IHEE} = \frac{E_{cl} - E_{ac}}{\dot{m} C_p (T_r - T_o)}. \quad (1)$$

The IHEE is positive (by analogy to heat exchanger effectiveness) when envelope heat recovery reduces the energy requirement due to infiltration.

If the IHEE is known, the air infiltration energy consumption (E_a) can be determined using Equation 2:

$$E_a = (1 - \text{IHEE})\, \dot{m} C_p (T_r - T_o). \quad (2)$$

However, there is no method available to calculate the IHEE of buildings from design data because it depends on the geometric forms of the cracks and on the airflow distribution, which cannot be determined from design data, as IHEE can only be determined from measurements at present.

Claridge and Bhattacharyya (1990) measured the IHEE of an indoor test cell under steady-state conditions. Later, Bhattacharyya and Claridge measured the IHEE of a frame wall section using a hot box facility (Bhattacharyya and Claridge 1992) under steady-state conditions. Liu and Claridge measured the IHEE of an outdoor test cell (Liu and Claridge 1992b) using a short-term average method (STAM) (Liu and Claridge 1993). All three experiments found values of IHEE that approached unity for conditions favorable to heat recovery and that were near zero (or even negative for the outdoor cell) for other conditions. This paper presents two methods suitable for measuring the IHEE in buildings in normal (nonsteady) environments. The co-heating and STAM approaches are both demonstrated using data from an outdoor test cell.

FUNDAMENTALS OF THE METHOD

Co-Heating Method

The co-heating method determines the IHEE using the measured average airflow rate and nighttime temperature difference between inside and outside with the room temperature and airflow rate held constant.

If the room temperature is kept constant, the energy balance equation of a building overnight can be expressed as

$$E_h = [UA_{wr} + (1 - \text{IHEE})\, \dot{m} C_p]\, \Delta T + E_{gr} - E_{so} + E_{st}. \quad (3)$$

Mingsheng Liu is assistant director and **David E. Claridge** is a professor and associate director of the Energy Systems Laboratory of the Mechanical Engineering Department at Texas A&M University, College Station.

Dividing both sides of Equation 3 by ΔT, it then follows that:

$$UA_{co} = UA_{wr} + (1 - \text{IHEE})\,\dot{m}C_p + UA_{gr} - UA_{so} + UA_{st} \quad (4)$$

where

$$UA_{co} = \frac{E_h}{\Delta T} \quad (5)$$

$$UA_{gr} = \frac{E_{gr}}{\Delta T} \quad (6)$$

$$UA_{so} = \frac{E_{so}}{\Delta T} \quad (7)$$

and

$$UA_{st} = \frac{E_{st}}{\Delta T}. \quad (8)$$

Note that if tests can be performed over a period of several days, when ambient temperature and solar radiation are relatively stable (all sunny days with daily average temperature differences less than 5°F), E_{gr}, E_{so}, E_{st}, and ΔT may have similar values for all tests. Consequently, it is assumed that UA_{gr}, UA_{so}, and UA_{st} can be treated as constants. Therefore, the energy balance equation may be rearranged as

$$UA_{co} = X_{co} + (1 - \text{IHEE})\,\dot{m}C_p \quad (9)$$

where X_{co} is the summation of UA_{wr}, UA_{gr}, UA_{st}, and $-UA_{so}$, which are generally constants and unknown.

According to the experimental results of Claridge and Bhattacharyya (1990) and the theoretical analysis of Liu and Claridge (1992c), when solar radiation is not present or is the same for all tests, the IHEE can be approximately expressed as

$$\text{IHEE} = a + b\frac{\dot{m}C_p}{UA_{wr}} \quad (10)$$

where a and b are two constants that vary with the airflow patterns and leakage configurations of buildings. Because UA_{wr} is a constant for a given building, Equation 10 may be written as

$$\text{IHEE} = a + b\dot{m}C_p. \quad (11)$$

Note that the constant a physically represents the value of IHEE when the airflow rate approaches zero. Therefore, it will differ according to airflow patterns and building leakage characteristics. Consequently, different test options are developed according to the value of a.

Option 1

If air infiltrates into a building through part of the envelope and exfiltrates through other parts (double flow), the IHEE approaches the maximum value of one when the airflow rate approaches zero. Therefore, Equation 11 then becomes

$$\text{IHEE} = 1 + b\dot{m}C_p. \quad (12)$$

To introduce Equation 12 into Equation 9, the energy balance equation becomes

$$UA_{co} = X_{co} - b\,(\dot{m}C_p)^2. \quad (13)$$

If two or more sets of measured data (airflow rate and UA_{co}) are available, the constants X_{co} and b can be determined according to Equation 13.

Note that because it is required that tests have similar temperature and solar radiation conditions in the building mass, tests should be performed on successive nights if ambient conditions are comparable. However, this requirement may result in similar airflow rates for all tests. Consequently, a small measurement error may result in a significant estimation error for b when Equation 13 is used.

Option 2

To overcome the difficulty noted in option 1, fans may be used to pressurize or depressurize buildings, so air is forced to leak out (or leak in) through the building envelope; this is called *single flow.* Under the single-flow pattern, the IHEE has a maximum value of 0.5 when the airflow rate approaches zero (Anderlind 1985; Liu and Claridge 1992c) because perfect heat exchange (IHEE = 1.0) is only possible when heat is recovered for both infiltration and exfiltration. Therefore, parameter a in Equation 11 becomes 0.5.

$$\text{IHEE} = 0.5 + b\dot{m}C_p. \quad (14)$$

Introducing Equation 14 into Equation 9, we get:

$$UA_{co} - 0.5\dot{m}C_p = X_{co} - b\,(\dot{m}C_p)^2. \quad (15)$$

If two data sets or more are available, then X_{co} and b can be determined according to Equation 15.

Because different airflow rates can be achieved by fans, this option can result in a good estimate of IHEE under the test conditions.

Option 3

Both option 1 and option 2 assume a maximum IHEE value when the airflow rate approaches zero. Because it is hard to perform tests with low airflow rates, treating parameter a as an unknown actually may improve IHEE estimation over the airflow range used in the tests.

Introducing Equation 11 in Equation 9 results in:

$$UA_{co} - \dot{m}C_p = X_{co} - a\dot{m}C_p - b(\dot{m}C_p)^2. \quad (16)$$

If three or more sets of data are available, X_{co}, a, and b can be determined by regression with Equation 17. Note that this option can be performed under both the single-flow and the double-flow patterns. This option requires at least one more test than Equation 15.

STAM Method

The co-heating method provides an easy way to measure IHEE during the night. However, the IHEE also is influenced by the interaction of solar radiation and air infiltration. To cover the impact of solar radiation, the STAM was developed to investigate air infiltration heat recovery (Liu 1992), including the solar interaction, and measure the heat loss factor of buildings (Liu and Claridge 1993). This method is modified here to measure the IHEE of buildings.

The STAM method requires tests to be performed with either constant room temperature or constant heat input over at least a two-day period. In addition, the airflow rate should be maintained constant for each test. "Zero net storage effect" periods are then chosen using three rules based on transfer function theory (Liu and Claridge 1993). These periods are chosen to have no net energy exchange with times outside the period, and span at least two nights and one day. Finally, the IHEE is determined using the average parameter values over these periods.

The first step is to measure the solar aperture with a three-day test under minimized airflow conditions. From this test, STAM can choose at least two "zero net storage effect" periods.

The energy balance equation over a "zero net storage effect" period can be expressed as shown in Equation 17 because the net thermal gain is zero:

$$E_h = [UA_{wr} + UA_{gr} + (1 - \text{IHEE})\dot{m}C_p]\Delta T - A_{so}I. \quad (17)$$

Because "zero net storage effect" periods generally cover a day or more, the UA_{gr} may be treated as constant. The IHEE also may be regarded as a constant for different "zero net storage effect" periods under natural conditions. Therefore, the three terms within the bracket can be considered as a constant, which is called the overall heat loss factor of the building, including the effects of air leakage:

$$UA = UA_{wr} + UA_{gr} + (1 - \text{IHEE})\dot{m}C_p. \quad (18)$$

Introducing Equation 18 into Equation 17, the energy balance equation is then:

$$E_h = UA\Delta T - A_{so}I. \quad (19)$$

The effective solar aperture (or "effective window" area, including solar gains from opaque surfaces) can be identified using Equation 19, according to the measured average heating input, the temperature difference, and the solar radiation.

The second step is to determine heat loss factors under different airflow rates and flow patterns. The heat loss factor of the building can be determined from a "zero net storage effect period" as

$$UA_{stam} = \frac{E_h + A_{so}I}{\Delta T}. \quad (20)$$

Finally, the relationship between IHEE and airflow rate must be determined. Combining Equations 18, 19, and 20, we get:

$$UA_{stam} = X_{stam} + (1 - \text{IHEE})\dot{m}C_p \quad (21)$$

where $X_{stam} = UA_{wr} + UA_{gr}$.

Option 1

For the single-flow pattern, assume

$$\text{IHEE} = 0.5 + b\dot{m}C_p. \quad (22)$$

Then Equation 22 can be written as

$$UA_{stam} - 0.5\dot{m}C_p = X_{stam} - b(\dot{m}C_p)^2. \quad (23)$$

If two or more sets of data are available, X_{stam} and b can be determined by using Equation 23.

Option 2

If IHEE is assumed to be

$$\text{IHEE} = a + b\dot{m}C_p \quad (24)$$

then Equation 21 can be written as

$$UA_{stam} - \dot{m}C_p = X_{stam} - a\dot{m}C_p - b(\dot{m}C_p)^2. \quad (25)$$

If three or more sets of data are available, the constants X_{stam}, a, and b can be determined by using Equation 25.

FACILITY AND MEASUREMENTS

The outdoor test cell was built in 1990 especially for the measurement of air infiltration heat recovery. The cell was a 2.4-m (8-ft) cube topped with a small attic. The walls were standard 5 cm by 10 cm (2 in. by 4 in.) frame construction with interior plywood sheathing, 10-cm fiberglass (R-11) insulation, and plywood. The ceiling and roof were built with plywood, 15-cm fiberglass (R-19) insulation, an attic air space, plywood sheathing, and asphalt roofing. The schematic of the test cell is shown in Figure 1.

There were two flow holes in the north wall (see Figure 2): hole A, which was 10 cm (4 in.) in diameter, served

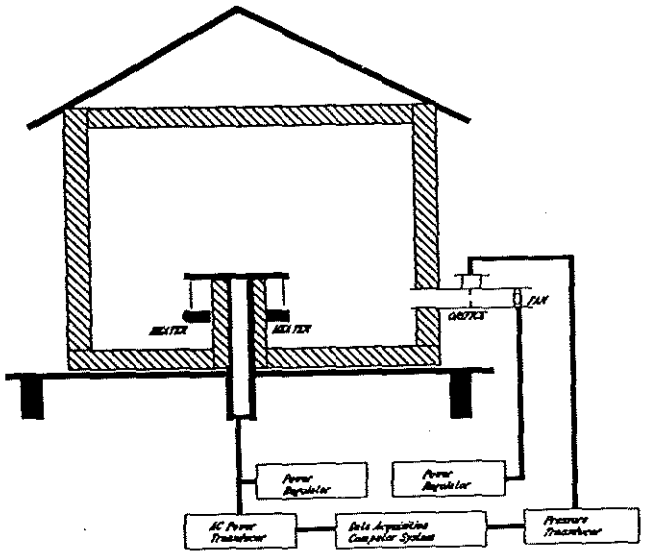

Figure 1 Schematic of the test cell.

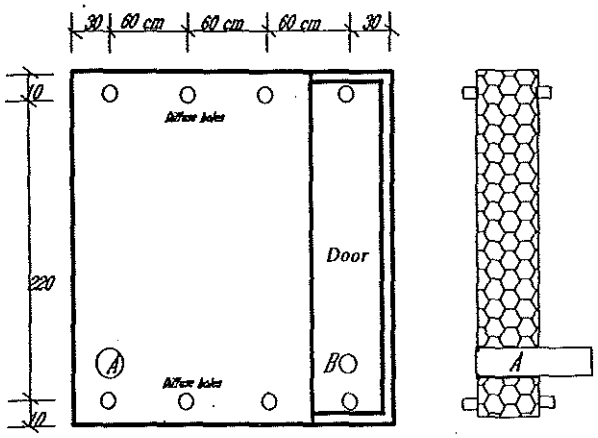

Figure 2 Schematic of the north wall.

as the fan outlet or inlet; hole B, which was 5 cm (2 in.) in diameter, served as a large or "concentrated" flow path. The north wall also contained a 61 cm (24 in.) wide by 205 cm (80 in.) high "door" to simulate crack flow. The construction of the "door" was similar to that of the wall. Both the interior and exterior plywood panels of each wall have eight "diffuse" holes (four located 13 cm [5 in.] from the ceiling, four located 13 cm [5 in.] from the floor) that are 1.3 cm (½ in.) in diameter and spaced at equal distances across the wall.

The test cell mass temperatures were monitored by 220 thermocouples (40 in each wall and floor and 20 in the ceiling). The test cell air temperature was monitored by 12 thermocouples that were uniformly distributed inside the cell space. The outside temperature was monitored by two well-shielded thermocouples located north of the cell. The horizontal solar radiation was measured by an on-site pyranometer, and the airflow rate was controlled by a fan with the flow rate measured by an orifice. The power was supplied by a heater with an adjustable range of 0 W to 500 W and was measured by a power transducer.

Table 1 Summary of the Sensors' Error Limits

Sensor	Unit	Sample Error	Measurement Error	Relative Error
Temperature	°C	0.50	0.10	0.3%
Power	W	5.0	1.0	0.3%
Airflow Rate	kg/s			3.0%
Pyranometer	W/m^2	5%		1.0%

The pressures across the walls, due to both natural forces and mechanically induced airflow, were measured separately by five pressure transducers (four for natural force, one for mechanical force).

A data-acquisition system was used to couple the sensors to a computer, where the signals were sampled, preprocessed, and finally recorded on a hard disk. All the signals were sampled every 10 seconds, and 10-minute time average values were recorded.

The error limits of sensors are summarized in Table 1. A temperature sample has an absolute error of 0.5°C, and an electricity sample has an absolute error of 5.0 W. An airflow sample has a relative error of 10%. The pyranometer has a relative error of 5%. These include errors from both the sensors and the data logger.

Because average values of measured samples were used in the data analysis, measurement errors were substantially smaller than sample errors according to ANSI/ASME PTC 19.1 Standard (ASME 1985). At least 72 samples were used to calculate the average parameters. The measurement error, then, can be calculated as $1/\sqrt{72}$ (1/8.5) of the sample error according to the ANSI/ASME standard. To be conservative, the measurement error was taken as one-fifth of the sample errors. The relative error values shown correspond to the measured values during the tests.

Four tests were performed with exfiltration at different airflow rates. The first test was conducted without airflow. The second, third, and fourth tests were conducted with airflow rates of 45, 68, and 71 kg/h, respectively. The first and second tests took four days each and the third and fourth took six days each.

The airflow rate, horizontal surface radiation, ambient temperature, heat input, and test cell temperature were measured by the data-acquisition system. The heat input to the test cell was kept at 250 W with maximum 10-minute data variation of ±5 W. The airflow rate was kept constant for each test with a maximum 10-minute data variation of 10%.

RESULTS AND DISCUSSION

Co-Heating Method

The co-heating method uses the average parameter values from midnight to 6 a.m. Because every test took more than one day, there was more than one set of data for each test. Table 2 summarizes the measured average

parameters from midnight to 6 a.m., which were used by the co-heating method. Column 1 lists the test number, and column 2 the date. Column 3 lists the test cell temperature (°C), column 4 the ambient temperature (°C), column 5 the airflow rate (kg/h), and column 6 the heat input (W) to the test cell.

The measured average parameters (Table 2) from midnight to 6 a.m. were used to identify the IHEE of the test cell according to the co-heating method. Because no double-flow test was performed, only co-heating options 2 and 3 were used. Table 3 summarizes the results for the co-heating method. Row 1 lists the case number representing data used in the analysis. Row 2 lists the test period that was used for IHEE identification for each case. For example, case 2 used three tests (test 2, test 3, and test 4). Row 3 lists the number of data sets used for regression. Rows 4 through 7 give the values of b, X_{co}, R-square, and CV (coefficient of variation) obtained by regression for option 2.

TABLE 2 **Measured Average Parameters from Midnight to 6:00 a.m.**

Test	Date	T_r (°C)	T_a (°C)	Air kg/h	Power (W)
1	08/23	29.5	16.6	0.0	207.8
	08/24	29.6	17.0	0.0	222.7
	08/25	30.0	17.9	0.0	201.7
	08/26	30.6	19.9	0.0	158.1
2	09/19	35.3	20.4	46.3	346.6
	09/20	35.4	20.7	45.0	332.4
	09/21	35.5	22.0	41.9	303.9
	09/22	34.3	16.4	43.2	463.7
3	09/24	27.7	12.3	67.9	478.3
	09/25	26.2	12.0	71.4	426.7
	09/26	27.2	15.8	66.9	268.3
	09/27	28.6	18.6	66.7	249.9
	09/28	26.2	12.7	67.3	392.7
	09/29	26.3	11.8	70.6	455.7
4	10/01	27.4	11.3	70.2	480.7
	10/02	25.7	11.2	71.3	429.8
	10/03	26.5	11.2	71.7	455.4
	10/04	26.5	11.0	70.9	441.0
	10/05	24.3	11.1	72.7	340.3
	10/06	25.7	13.8	72.9	331.2

Table 3 **Results of IHEE Identification Using Co-Heating Method**

Case		1	2	3	4	5
Tests		1,2,3,4	2,3,4	2,3	3,4	2,4
Data Sets		20	16	10	12	10
Option 2	b	-0.00591	-0.00535	-0.00764	-0.01589	-0.00347
	X_{co}	16.35	16.55	16.05	12.44	17.00
	R-square	0.195	0.065	0.112	0.0269	0.0711
$\varepsilon = 0.5 + bmc_p$	CV	0.03	0.03	0.03	0.04	0.03
	a	0.471	2.321			
Option 3	b	-0.00458	-0.06167			
	X_{co}	16.29	30.52			
	R-square	0.695	0.214			
$\varepsilon = 0.5 + bmc_p$		0.04	0.06			

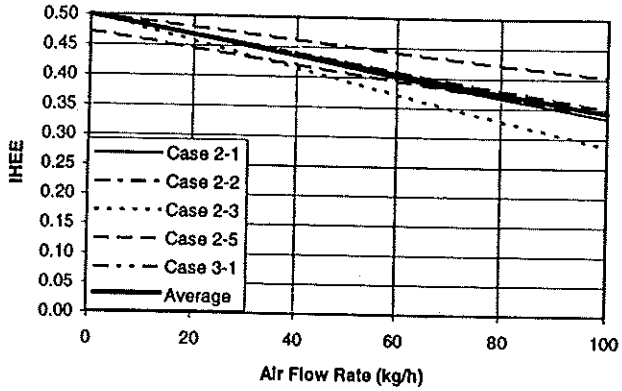

Figure 3 *IHEE vs. airflow rate from co-heating identification.*

It may be noted that case 4 has an estimated X_{co} value of 12.44, which is 24% smaller than the median value (16.35). The value of X_{co} should be close to the total heat transfer coefficient of the test cell, which is calculated as 17.7 W/°C. Because the airflow rate of test 3 is only 4% smaller than that of test 4, which is just above the measurement uncertainty of 3%, the results of this case were ignored.

After rejecting case 4, the value of b varies from -0.00347 to -0.00764, with an average of -0.00559. The negative values infer that the IHEE decreases with airflow rate. This is expected from basic heat transfer theory, because effectiveness decreases at higher flow rates.

Rows 8 through 12 show the results of option 3. Note that option 3 can only have results for cases 1 and 2 because three tests are required to estimate three parameters. Case 1 results in reasonable estimates of a and b. However, case 2 estimated a as 2.3, which is far from the expected value of 0.5. The poor results from case 2 may be due to the similar airflow rates for tests 3 and 4.

The values of IHEE were generated using the values of a and b identified in different cases. Figure 3 shows IHEE as a function of airflow rate for cases 1, 2, 3, and 5 of option 2, case 1 of option 3, and their average value. Clearly, cases 1 and 2 of option 2 and case 1 of option 3 show close agreement in values (within 0.01) of IHEE. In these cases, the number of tests is larger than the degree of freedom (number of parameters estimated), while cases 3 and 5 of option 2 have relatively large bias and the number of tests used for regression equals the regression degree of freedom. It appears that option 2 provides better estimates of IHEE when using at least three tests than when using two tests and option 3 can provide better estimates of IHEE when using at least four tests than when using three tests.

STAM Method

Table 4 summarizes measured average parameters over "zero net storage effect" periods, which were chosen by the STAM method (Liu and Claridge 1993). The "zero net storage effect" periods generally spanned two nights. Column 1 lists the test number, column 2 the test cell temperature (°C), column 3 the ambient temperature (°C), column 4 the solar radiation (W/m^2), column 5 the heat input (W), and column 6 the airflow rate (kg/h). Note that the solar radiation values are the average incident solar radiation on the unit test cell surface calculated by an ASHRAE model from measured horizontal solar radiation (Liu 1992).

The measured average parameters (Table 4) over the "zero net storage effect" periods were used to identify the solar aperture and the IHEE of the test cell according to the STAM method. The solar aperture was identified as 0.04117 W/W_{so} using data from test 1 according to Equation 19.

Table 5 summarizes the results of IHEE from the STAM method. Row 1 lists the case number. Row 2 lists the tests that were used for IHEE identification for each analysis or case. Row 3 lists the number of data sets used for the regression. Rows 4 through 7 give the values of the

TABLE 4 **Measured Average Parameters Over "Zero Net Storage Effect" Periods**

Test	T_{cell}	T_a	Solar (W/m^2)	Power (W)	Air (kg/h)
	29.5	22.4	61.6	135.2	0
1	29.5	23.0	63.6	119.4	0
	29.6	23.5	64.8	105.6	0
2	34.7	24.3	70.7	275.0	44.4
	34.6	24.2	73.1	268.8	43.7
3	28.1	20.8	66.3	208.2	67.0
	25.4	17.2	88.8	278.9	71.3
4	25.4	17.3	87.8	271.5	71.3
	25.3	17.6	90.8	253.3	71.3
	25.3	17.7	87.9	254.5	71.3

Table 5 **Results of IHEE Identification Using STAM Method**

Case		1	2	3	4	5
Tests		**1,2,3,4**	**2,3,4**	**2,3**	**3,4**	**2,4**
Data Sets		**10**	**7**	**3**	**5**	**6**
Option 1	b	0.01164	-0.01282	0.00297	-0.08602	0.01406
	X_{stam}	18.24	17.81	20.51	-11.09	17.90
	R-square	0.770	0.562	0.487	0.962	0.958
$\varepsilon = 0.5+bmc_p$	CV	0.02	0.02	0.11	0.01	0.01
Option 2	a	0.5898				
	b	0.01595				
	X_{stam}	18.37				
$\varepsilon = 0.5+bmc_p$	R-square	0.829				
	CV	0.02				

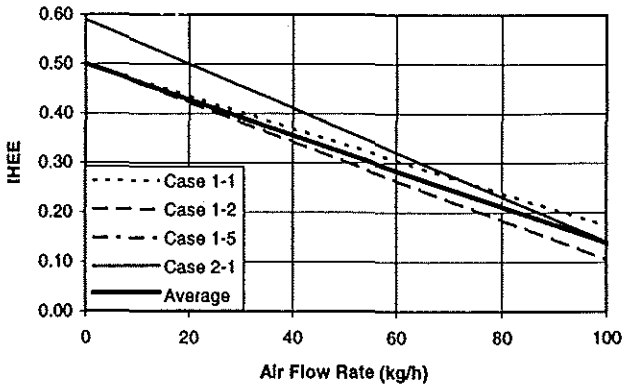

Figure 4 *IHEE vs. airflow rate for STAM identification.*

constants b, X_{stam}, R-square, and CV from the regression for option 1, where the air infiltration heat recovery was assumed to be

$$\text{IHEE} = 0.5 + b \times \dot{m}C_p. \quad (26)$$

It may again be noted that case 4 has an estimate of X_{stam} as –11.09. Actually, the X_{stam} should equal the total heat transfer coefficient, which is 18.0 W/°C. The result of this case was considered invalid. It was also noticed that case 3 has a positive estimate of the constant b, where the number of data sets for regression equals the number of regression degrees of freedom. Because it is impossible to have a positive value of b, case 3 also is considered invalid.

After rejecting cases 3 and 4, b varies from –0.01164 to –0.01406, with an average value of –0.01284. The negative values infer that the IHEE decreases with airflow rate.

Rows 8 through 12 show the results of option 2. The constants a, b, and X_{stam} were determined properly.

The values of IHEE were generated using the values of a and b identified in the different cases. Figure 4 shows the IHEE as a function of airflow rate for cases 1, 2, and 5 of option 1; case 1 of option 2; and their average value. All cases provided similar IHEE values (within 0.1). It seems that option 1 of the STAM method can provide better estimates of IHEE when using three tests than when using two tests.

Comparison of the Co-Heating and STAM Methods

Figure 5 compares the results identified using both the co-heating and STAM methods. The values of IHEE were generated using the average values of parameters estimated from cases 1, 2, 3, and 5 of option 2 for co-heating, and the average from cases 1, 2, and 5 of option 1 for STAM. Figure 5 shows that the IHEE estimated by the STAM method is smaller than that estimated by the co-heating method, and the difference increases as the airflow rate increases. Note

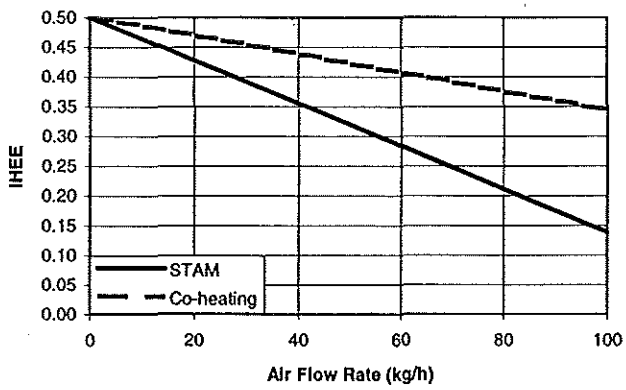

Figure 5 *IHEE comparison of the co-heating and STAM methods.*

that STAM identifies the IHEE of the "zero net storage effect" period, which includes daytime hours, while the co-heating estimate of IHEE includes only nighttime hours. Because the tests were performed under exfiltration flow conditions and some of the absorbed solar energy was rejected to the outside, the value of IHEE from the "zero net storage effect" periods should be smaller than that from nighttime periods. Consequently, the difference between the co-heating and STAM estimations may be considered as due to the effects of the interaction between solar radiation and air infiltration.

Table 6 summarizes the results of X_{co} and X_{stam}. It is found that the values of X_{stam} are larger than those of X_{co}. After rejecting case 4, the average value (18.62) of X_{stam} is 1.13 times the average value of X_{co} (16.49).

Note that X_{co} is the sum of UA_{wr} (heat loss factor of envelope), UA_{gr}, $-UA_{so}$, and UA_{sl} (see Equation 6, 7, 8, and 9) while X_{stam} is the sum of UA_{wr} and UA_{gr}. Because the test cell has no ground heat transfer, X_{co} is the sum of UA_{wr} and correction terms due to the thermal storage effect caused by solar radiation, as well as the relatively higher temperature during the daytime, and X_{stam} is UA_{wr}. Therefore, the difference of X_{co} and X_{stam} represents the impact of the thermal storage effect due to solar radiation and the relatively higher daytime temperature. Clearly, the lower value of X_{co} indicates that the solar radiation and relatively higher daytime temperature contribute heat gain to the test cell later at night. However, the co-heating method can properly identify IHEE using short-term measured data at night and rejects the effects of thermal storage automatically to X_{co}.

The values of R-square and the coefficient of variation (CV) are summarized in Table 7. The values of the R-square from the STAM method are much higher than those from the co-heating method. The CV values from the STAM method are much lower than those from the co-heating method. It seems that the results from the STAM have better accuracy and confidence than those from the co-heating method.

Table 6 **Summary of Regressed Constants X_{co} and X_{stam}**

Case	1	2	3	4	5
Tests	1,2,3,4	2,3,4	2,3	3,4	2,4
X_{co}	16.35	16.55	16.05	12.44	17.00
X_{stam}	18.24	17.81	20.51	−11.09	17.90

Table 7 **Summary of Correlation Factors or R-square from Both the Co-Heating and STAM Methods**

Case		1	2	3	4	5
Tests		1,2,3,4	2,3,4	2,3	3,4	2,4
Co-heating	R-square	0.195	0.065	0.112	0.026	0.071
	CV	0.03	0.03	0.03	0.04	0.03
STAM	R-square	0.770	0.562	0.487	0.962	0.958
	CV	0.02	0.02	0.11	0.01	0.01

Note that the higher R-square of the STAM method may be partially due to the higher gradient of Equations 27 and 29 and the fewer data sets used for the regression. The co-heating method requires (see "Fundamental Theory" section) constant thermal effect terms for all tests; however, the tests were performed under quite different weather conditions. For example, the ambient temperature was about 18°C for the first test, 20°C for the second test, 13°C for the third test, and 11°C for the last test. This inconsistency may partially account for the lower correlation factor value from the co-heating method. The co-heating method may have resulted in better estimations if the tests had been performed under similar weather conditions.

CONCLUSION

Two methods have been developed in this paper for measuring the air infiltration heat exchange effectiveness. Both the co-heating and STAM methods can be used to determine IHEE through short-term tests.

When IHEE can be taken as 0.5 in the zero-flow limit, both the co-heating and STAM can determine parameter b using three tests; when the IHEE value in the zero-flow limit needs to be estimated, four tests are required to determine a and b by both the STAM and co-heating methods. Note that a co-heating test takes a few hours at night, while a STAM test takes at least two days.

Note that both the methodology and the test verification presented in this paper are preliminary. A number of assumptions, based on the authors' experiences, are the subject of detailed study and investigation.

NOMENCLATURE

a = constant
A = area (m^2)
b = constant
C_p = specific heat of air (J/kg·K)
E = energy consumption (W)
I = average solar radiation on the building envelope (W/m^2)

IHEE= air infiltration heat exchange effectiveness
$\dot{m}$ = air infiltration rate (kg/s)
n = exponent of the power law
Q = total infiltration (m^3/s),
T = temperature (°C)
UA = heat loss factor of a building (W/K)
ΔP = pressure difference (Pa)

Subscripts

a = air
ac = actual
cl = classic
co = co-heating
gr = ground
h = heating
o = outside
r = room
so = solar
st = storage
$stam$ = short-term average method
wr = wall and roof

REFERENCES

Anderlind, G. 1985. Energy consumption due to air infiltration. *Proceedings of the 3rd ASHRAE/DOE/BTECC Conference on Thermal Performance of the Exterior Envelopes of Buildings*, Clearwater Beach, Fla., pp. 201-208.

ASHRAE. 1993. *1993 ASHRAE handbook—Fundamentals*. Atlanta, Ga.: American Society of Heating, Refrigerating and Air-Conditioning Engineers, Inc.

ASME. 1985. *ANSI/ASME PTC 19.1-1985, Measurement uncertainty*. New York, N.Y.: American Society of Mechanical Engineers.

Bhattacharyya, S., and D.E. Claridge. 1992. The energy impact of air leakage through insulated walls. *Proceedings of 1992 ASME Solar Energy Division Conference*, Miami, Fla. New York, N.Y.: American Society of Mechanical Engineers.

Claridge, D.E., and S. Bhattacharyya. 1989. The measured energy impact of infiltration in a test cell. *Solar Engineering—1989 Proceedings of the 11th Annual ASME Solar Energy Conference*, San Diego, Calif.

Claridge, D.E., and S. Bhattacharyya. 1990. The measured energy impact of infiltration in a test cell. *Journal of Solar Energy Engineering* 112: 123-136.

Guo, J., and M. Liu. 1985. The energy saving effect of double frame windows. *Proceedings of the CLIMA 2000 World Congress on Heating Ventilating and Air-Conditioning*, vol. 2, Copenhagen, Denmark.

Liu, M. 1992. Study of air infiltration energy consumption. Ph.D. Dissertation. College Station: Texas A&M University.

Liu, M., and D.E. Claridge. 1992a. The measured energy impact of infiltration under dynamic conditions. *Proceedings of the 8th Symposium on Improving Building Systems in Hot and Humid Climates*, Dallas, Texas.

Liu, M., and D.E. Claridge. 1992b. The measured energy impact of infiltration in an outdoor test cell. *Proceedings of the 8th Symposium on Improving Building Systems in Hot and Humid Climates*, Dallas, Texas.

Liu, M., and D.E. Claridge. 1992c. The energy impact of combined solar radiation/infiltration/conduction effects in walls and attics. *Proceedings of Thermal Performance of the Exterior Envelopes of Buildings, 5th ASHRAE/DOE/BTECC Conference*, Clearwater Beach, Fla.

Liu, M., and D.E. Claridge. 1993. A calorimetric method for heat transfer coefficient identification of thermal enclosures. *Solar Engineering 1993, Proceedings of the ASME International Solar Energy Conference*, Washington, D.C., April 4-9, pp. 493-505.

Morrison, I.D., A.N. Karagiozis, and K. Kumaran. 1992. Thermal performance of a residential dynamic wall. *Proceedings of Thermal Performance of the Exterior Envelopes of Buildings, 5th ASHRAE/DOE/BTECC Conference*, Clearwater Beach, Fla.

Timusk, J., and H.B. Doshi. 1986. Effect of insulating sheathing on heat and moisture flow. *Canadian Journal for Civil Engineering* 13.

Timusk, J., A.L. Seskus, and K. Linger. 1992. A systems approach to extend the limit of envelope performance. *Proceedings of Thermal Performance of the Exterior Envelopes of Buildings, 5th ASHRAE/DOE/BTECC Conference*, Clearwater Beach, Fla.

Virtanen, M., I. Heimonen, and R. Kohonen. 1992. Application of the transfer function approach in the thermal analysis of dynamic wall structures. *Proceedings of Thermal Performance of the Exterior Envelopes of Buildings, 5th ASHRAE/DOE/BTECC Conference*, Clearwater Beach, Fla.